Contents lists available at ScienceDirect

Applied Catalysis B: Environmental

Decomposition of perfluorooctanoic acid photocatalyzed by titanium dioxide: Chemical modification of the catalyst surface induced by fluoride ions

Maurizio Sansotera [a,b,c,*], Federico Persico [b,c], Carlo Pirola [a,b], Walter Navarrini [b,c], Alessandro Di Michele [c,d], Claudia L. Bianchi [a,b]

[a] Dipartimento di Chimica, Università degli Studi di Milano, Via Golgi 19, 20133, Milano, Italy
[b] Dipartimento di Chimica, Materiali e Ingegneria Chimica "Giulio Natta", Politecnico di Milano, Via Mancinelli 7, 20131, Milano, Italy
[c] Consorzio Interuniversitario Nazionale per la Scienza e Tecnologia dei Materiali, Via G. Giusti 9, 50121 Firenze, Italy
[d] Dipartimento di Fisica, Università di Perugia, Via Pascoli, 06123 Milano, Perugia, Italy

ARTICLE INFO

ABSTRACT

The degradation of perfluorooctanoic acid (PFOA) in water was investigated both as photolysis and photocatalysis by slurry titanium dioxide. Different surfactant concentrations, the catalyst nature and concentration as well as the irradiation power of the UV lamp were evaluated. The reactions were conducted using merely the natural dissolved oxygen (DO), in order to simulate conditions of non-enriched water, as industrially feasible. The photomineralization of PFOA was monitored by total organic carbon (TOC) analysis and ionic chromatography (IC). Finally, the photocatalytic powder was analyzed at different reaction times by X-ray photoelectron spectroscopy (XPS) and by X-ray powder diffraction (XRD) technique in order to study and interpret the catalyst deactivation phenomena occurred during the treatment.

1. Introduction

The production of surfactants is nowadays estimated at around 15 Mton/y, about half of which are soaps like linear alkyl-benzene sulfonates, lignin sulfonates, fatty alcohol ethoxylates and alkylphenol ethoxylates [1]. Surfactants are employed in extremely different fields, such as textile, food, paint, polymer, cosmetic, pharmaceutical, microelectronic, mining and oil recovery [1]. However, these compounds are among the most widely diffused xenobiotic substances that can be found into waste streams and are responsible for polluting the aquatic environment [2–4]. They are the main cause of foam production in rivers and lakes, reducing overall the water quality [1,3,4]. For these reasons, the regulatory authorities, such as the United States Environmental Protection Agency (US-EPA) and the European Environment Agency (EEA), fixed strict limitations on the environmental surfactants concentration [5–7].

Surfactants are normally removed from water by using the activated sludge techniques, but their complete elimination cannot be guaranteed. Other traditional removal methods for such contaminants include biological processing, chemical treatment, incineration, air stripping followed by carbon adsorption and landfilling [1,8]. However, adsorption and landfill merely transfer the contaminant to a different phase or location that requires secondary disposal treatments, while incineration can cause the generation of potentially pollutant or toxic compounds that must be destroyed through a dedicated processes. On the other hand, biodegradation is very sensitive to many environmental factors, such as pH, temperature, aeration, nature and concentration of the pollutant and the presence of other toxic compounds (e.g. cyanides, phenols, formaldehyde, pesticides and heavy metals like Cd, Hg, Pb, Ni and Cr) [8,9]. However, the biodegradative techniques show low degradation rates, often produce unpredictable results and are inefficient for highly concentrated waste effluents. For these reasons, advanced oxidation processes (AOPs) are used as alternative methods in the degradation of surfactants and, generally, for wastewater treatments. The AOPs mechanism is generally based on reactions generating hydroxyl radicals (HO·), which have high redox potential ($E_0 = 2.73$ V) and consequently can non-selectively react with any organic compound [10,11]. Hydroxyl radicals are generated by using one or more primary oxidants, such as ozone, hydrogen peroxide or oxygen, and/or energy sources, like ultraviolet radiations, or through a catalyst, such as titanium dioxide [12,13].

* Corresponding author. Tel.: +39 02 2399 3035, fax: +39 02 2399 3180.
E-mail address: maurizio.sansotera@polimi.it (M. Sansotera).

Semiconductor photocatalysis offers convenient routes to decontamination of air and water from gaseous, dissolved or solid compounds, even if present in low concentrations [14–16]. Such materials are able to photocatalyze the complete mineralization of many organics, including aromatics, insecticides, pesticides, dyes, surfactants, hormones and halohydrocarbons [17–20], through an overall process that can be summarized as follows:

$$Organic pollutant + O_2 \rightarrow mineralized products \qquad (1)$$

Photocatalytic reactions take place over the photocatalyst surface and in semiconductors like titanium dioxide the exposure to radiations energetically higher than band-gap generates an electron–hole pair that can either recombine or react with adsorbed species [11,16,21,22]. The photogenerated electrons are capable to reduce surface oxygen to water, while the photogenerated holes can mineralize organic compounds [11,16,21,22]. The oxidation process is probably due to the initial oxidation of surface OH^- groups to reactive $OH \cdot$ radicals which subsequently oxidize the adsorbed organic species [11,22,23].

Perfluorocarboxylic acids (PFCAs) are a class of fully fluorinated carboxylic acids, industrially employed as surfactants and fire retardants [3,7,24,25]. Within the PFCA class, perfluorooctanoic acid, $C_8HF_{15}O_2$ (AMW = 414.07 g/mol), is one of the most widespread industrial surfactants [1,24,26]. It is mostly utilized in the synthetic route of polytetrafluoroethylene (PTFE), polyvinylidene fluoride (PVDF) and fluoroelastomers as surfactant in the emulsion polymerization process [27–29]. PFOA is also used as insulator for electric wires, in planar etching of fused silica [30], in fire-fighting foams [31] and in outdoor clothing [32]. It has been found to be bioaccumulative [2,24], carcinogen [26], liver and immune system toxicant and able to exert hormonal effects, including alteration of thyroid hormone levels [29,33]. Moreover, it has been associated with signs of reduced fetal growth including low birth weight [34–36]. Because of the typical chemical, thermal and photochemical stability of perfluorinated compounds due to the highly energetic C–F bonds (which ranges as high as 130 kcal/mol) [18,37,38], PFOA is slowly degraded by means of standard techniques and the advanced oxidation processes (AOPs) are preferred as alternative methods.

In the present paper, the photomineralization of PFOA by a commercial titanium dioxide (P25 by Evonik®) was tested in different conditions and monitored by Total Organic Carbon (TOC) analysis and ionic chromatography (IC). TOC analysis determined the trend of the carbon content in solution and IC measured the amount of fluoride ions generated during the PFOA abatement [2,39,40]. The photocatalyst was analyzed at different reaction times by both X-ray photoelectron spectroscopy (XPS) and by X-ray powder diffraction (XRD) techniques to evaluate the variations during the treatment.

2. Materials and methods

2.1. Materials

Perfluorooctanoic acid (purity 96% — from Sigma Aldrich®) was used as received. PFOA is soluble in water (9.5 g/L) and its critical micelle concentration (CMC) is 7.80×10^{-3} mol/L at 25 °C [6]. Titanium dioxide P25 (75% Anatase, 25% Rutile [41]) was supplied by Evonik® and it was tested as titanium-based photocatalyst. Water was purified using an Elga Option 3 deionizer and was used to prepare all solutions. Milli-Q water was employed for ion chromatography. Fluorinated titanium compounds TiF_3, TiF_4 and K_2TiF_6 (Sigma Aldrich®) were used as received as reference materials for F 1s and C 1s XPS Binding Energy values.

2.2. Photocatalysis

The apparatus for photocatalysis was a 1 L glass stirred reactor equipped with a low-pressure mercury UV lamp (500 W, Jelosil® HG500) emitting light at wavelengths of 310–400 nm and able to irradiate the reactor with a specific power of 75 or 95 W/m². The UV lamp was placed beside the reactor, which was cooled with water at a temperature of 30 ± 5 °C [42]. A stock solution of PFOA (0.1 M) was prepared and diluted to chosen concentrations. Titanium dioxide was introduced in the reactor at the beginning of each test. For each experiment, the variation of the surfactant concentration in solution was monitored by TOC analysis and IC. Samples (10 ml) of the reaction mixture were collected at different reaction times for the analyses: typically at 0 min (before the start of the reaction), 30 min, 60 min, 120 min, 180 min, 240 min and 300 min. Each sample of the reaction mixture was centrifuged and filtered through a 0.45 μm polycarbonate membrane in order to separate the TiO₂ powder from the solution.

The degradation reaction of perfluorooctanoic acid was evaluated comparing the effects of photolysis and photocatalysis, employing different surfactant concentrations: 0.0040 M (below the CMC), 0.0078 M (at the CMC) and 0.0120 M (above the CMC). The catalyst concentration (0.66 g/L; 1.00 g/L) and the irradiation power of the UV lamp (75 W/m²; 95 W/m²) were varied to test the degradation reaction in different conditions. For comparison, the reaction was also tested in presence of TiO₂ as photocatalyst (0.66 g/L) but without UV irradiation (dark test).

Photocatalysis follows the Langmuir–Hinshelwood model [43]. When the PFOA adsorption onto the photocatalyst surface is negligible, the reaction mechanism can be approximated to a pseudo-first order kinetic (2):

$$r = -\frac{dC}{dt} = k_{app}C \qquad (2)$$

In Eq. (2), r is the reaction rate, C is the surfactant concentration in solution, t is the time and k_{app} the apparent first order rate constant. The data obtained by TOC analysis were considered for calculation of kinetic parameters (Supplementary information Table 1). The reactions were conducted without a constant feed of oxygen as reported by Li et al. [44], but using just the naturally dissolved O₂ (DO), in order to simulate conditions of non-enriched water, as industrially feasible.

2.3. TOC analysis and ion chromatography

The total organic carbon (TOC) analysis allowed to evaluate and to monitor the trend of the carbon content of the solution. TOC analyses were performed with a Shimadzu® TOC 5000 A with a combustion/non-dispersive infrared (NDIR) gas analysis method. The total organic carbon concentration of the PFOA solution at different photodegradation times was calculated automatically comparing the sample with a calibration curve obtained from solutions of PFOA at known concentrations. In the kinetic study of PFOA degradation, the data obtained by TOC analysis were considered for the calculation of C/C_0 ratios.

The PFOA degradation generated fluoride ions in solution and their concentration was monitored by ion chromatography with a Metrohm 883 Basic IC Plus.

2.4. X-ray photoelectron spectroscopy (XPS)

X-ray photoelectron spectroscopy analysis was performed to study the photocatalyst surface before and after the photodegradation reaction, in order to monitor composition variations that might have occurred. X-ray photoelectron spectroscopy spectra were obtained by using an M-probe apparatus (Surface Science

Instruments). The source was monochromatic Al Kα radiation (1486.6 eV). A spot size of 200 μm × 750 μm and pass energy of 25 eV were used. 1s level hydrocarbon-contaminant carbon was taken as the internal reference at 284.6 eV. Fittings were performed using pure Gaussian peaks, Shirley's baseline, and without any constraints. Samples for XPS analysis were obtained centrifuging and filtering through a 0.45 μm polycarbonate membrane the surfactant solution at different reaction times (2 h, 4 h, 9 h); the samples were then dried in inert atmosphere for 24 h and analyzed. Subsequently, in order to remove possible fluorinated organic compounds deposited on the catalyst surface, the samples were suspended in the fluorinated solvent $CF_3OCFClCF_2Cl$, dried in inert atmosphere and analyzed again.

For each sample, survey analyses in the whole range of X-ray spectra and high resolution analyses in the typical zone of C-1s, Ti-2p, O-1s and F-1s were performed.

2.5. X-ray diffraction (XRD)

XRD powder patterns were obtained on a X'Pert Pro PANalytical diffractometer with Cu-Kα radiation at a scan rate of 0.03° s^{-1}. Rietveld method with GSAS software was used in order to determine the crystallite size in the samples. The peak shape in profile refinements was described by a pseudo-Voigt function.

2.6. Fourier transform infrared spectroscopy (FT-IR)

Infrared spectra were measured with an FT-IR model tensor 27 Bruker spectrometer, with resolution of 1 cm^{-1} in the spectral region 1000–2000 cm^{-1}. KBr pellets of different thicknesses were prepared in order to obtain the best signal/noise ratio. Photocatalyst samples for FT-IR analysis were obtained as described for XPS analysis in paragraph 2.7.

3. Results and discussion

3.1. Photocatalysis results

The PFOA total degradation reaction in water could be written on the base Equation (1) as follows:

$$CF_3(CF_2)_6COOH + 7/2O_2 + 7H_2O \rightarrow 8CO_2 + 15HF \quad (3)$$
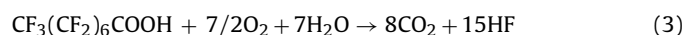
The photocatalytic mechanism is still not totally explained, particularly with regard to the role played by oxygen [11,45]. Concerning the oxidation mechanism, it is generally accepted that many compounds generated by oxygen reduction, such as HO$_2$·, HO$_2^-$, H$_2$O$_2$ and above all OH·, being strong oxidizers, are fundamental for the oxidation of organics; on the other hand, it has been also demonstrated that Ti^{IV}OH·$^+$ has an essential role in the mineralization reaction, as reported by Mills and Le Hunte [11,46,47]. Furthermore, it has been shown that the oxidation reaction requires firstly the oxidation of surface hydroxyl groups to hydroxyl radicals OH·, which subsequently interact with the organics, oxidizing them [11,22]. Still it is not clear if the oxidation of the organic is due to a direct reaction with the photogenerated holes, to an indirect reaction with hydroxyl radicals or to a combination of the two [18].

The proposed PFOA degradation mechanism is initiated with the excitation of titanium dioxide caused by the irradiation of UV light [11,22,48]; excited TiO$_2$ accepts one electron from dissociated PFOA (CF$_3$(CF$_2$)$_6$COO$^-$), generating PFOA radical (4) [11,22,48]. As clarified in various papers, PFOA decomposition starts in correspondence to the carboxylic function [2,48–50]. The so-formed species undergo Kolbe decarboxylation reaction (5) [39,48].
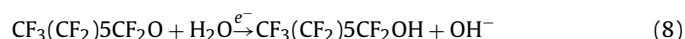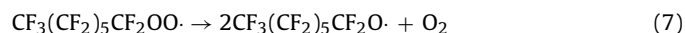
$$CF_3(CF_2)_6COO^- \xrightarrow{h^+} CF_3(CF_2)_6COO \cdot \quad (4)$$

$$CF_3(CF_2)_6COO \cdot \rightarrow CF_3(CF_2)_5CF_2 \cdot + CO_2 \quad (5)$$
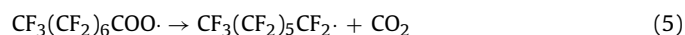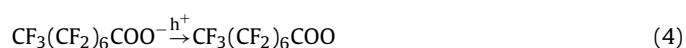
The C$_7$ radicals can subsequently react with molecular oxygen present in the reaction environment to generate the peroxoradical (6) [40]:

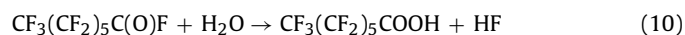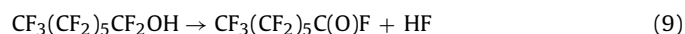$$CF_3(CF_2)_5CF_2 \cdot + O_2 \rightarrow CF_3(CF_2)_5CF_2OO \cdot \quad (6)$$
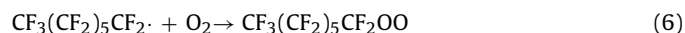
Alternatively, C$_7$ radicals can incur in coupling reactions that cause the formation of fluorinated alkanes.

The coupling of two peroxoradicals allows the production of oxoradicals (7) that in presence of the surface excited electrons of TiO$_2$ and water generate an unstable primary perfluorinated alcohol (8) [40,51].

$$CF_3(CF_2)_5CF_2OO \cdot \rightarrow 2CF_3(CF_2)_5CF_2O \cdot + O_2 \quad (7)$$

$$CF_3(CF_2)5CF_2O + H_2O \xrightarrow{e^-} CF_3(CF_2)5CF_2OH + OH^- \quad (8)$$

Primary perfluorinated alcohols are thermodynamically unstable and originate the corresponding acyl fluorides and hydrogen fluoride (9) [39,51]; in presence of water, the so formed acyl fluoride hydrolyzes to the carboxylic acid (10) [39,51–55].

$$CF_3(CF_2)_5CF_2OH \rightarrow CF_3(CF_2)_5C(O)F + HF \quad (9)$$

$$CF_3(CF_2)_5C(O)F + H_2O \rightarrow CF_3(CF_2)_5COOH + HF \quad (10)$$

This mechanism explains the C$_n \rightarrow$ C$_{n-1}$ chain length decrease during PFOA degradation. It has been verified by Panchangam et al. and crosschecked by HPLC-MS analyses which detected PFCAs with shorter carbon chain length, like perfluoroheptanoic acid (PFHpA), perfluorohexanoic acid (PFHxA), perfluoropentanoic acid (PFPeA), perfluorobutanoic acid (PFBA), perfluoropropanoic acid (PFPrA) and trifluoroacetic acid (TFA) [48].

The surfactant abatement trends were monitored studying the percentage mineralization of PFOA and the fluoride concentrations at different times. In Fig. 1A, the kinetic curves of PFOA photodegradation reaction with of TiO$_2$ as photocatalyst, under UV irradiation of 75 W/m^2 and at different surfactant concentrations (4.0 mM, 7.8 mM and 12.0 mM) are reported. The corresponding linearization curves are shown in Fig. 1B.

The reaction kinetics appeared to follow a pseudo-first order trend (correlation coefficient $R^2 > 0.94$), which enabled the comparison of rate constants. Three different values of the apparent kinetic constant (k_{app}) were observed changing the surfactant concentration in solution; working with PFOA at 0.0120 M, 0.0078 M and 0.0040 M, the calculated k_{app} were equal to 0.0332 h^{-1}, 0.0493 h^{-1} and 0.0572 h^{-1}, respectively. Thus, the highest degradation rate was obtained when the PFOA concentration was the lowest. The mineralization data after 6 h revealed that the mineralization ratios were 17%, 24% and 30% with PFOA at 0.0120 M, 0.0078 M and 0.0040 M, respectively. A similar trend was observed for the fluoride concentration in solution, whose increase was directly proportional to the decrease of PFOA: theoretically, 15 moles of fluoride ions are released as a result of the complete mineralization of each PFOA mole. In particular, the fluoride content of the different solutions appeared to be minimum at PFOA 0.0120 M (10% after 6 h), at 0.0078 M a higher content of fluoride ions was measured (16% after 6 h), while at 0.0040 M the maximum concentration of fluorides was observed (22% after 6 h). The yield in fluoride ions (calculated as the ratio of the concentration of fluoride ions over the initial concentration of PFOA multiplied by 15) was lower than the PFOA mineralization values. The adsorption of fluoride ions on the particles of TiO$_2$ might be a probable reason of the fluoride ions loss in the aqueous phase. As reported in Supplementary information Table 1, no PFOA abatement was observed working in presence of TiO$_2$ as photocatalyst (0.66 g/L) without UV irradiation
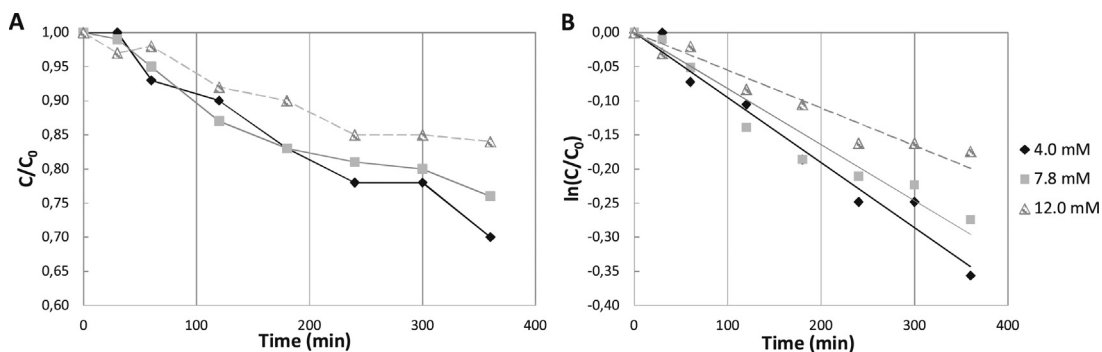
Fig. 1. Kinetic curves—PFOA degradation (A) at different concentrations (4.0 mM, 7.8 mM and 12.0 mM) and linearization (B) based on a pseudo-first order kinetic. TiO$_2$ content 0.66 g/L; UV irradiation 75 W/m^2.
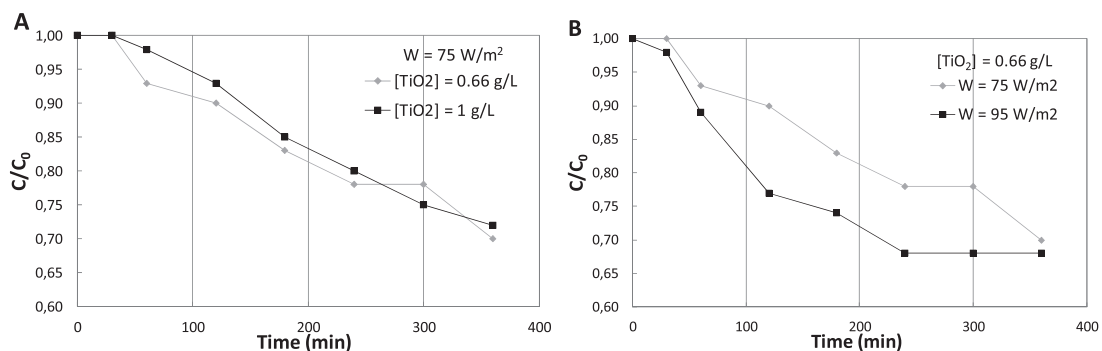

Fig. 2. Kinetic curves—Photodegradation of 4.0 mM PFOA solutions (A) with different contents of titanium dioxide and (B) under irradiation with different UV lamp specific power.

(dark test) or working just under UV irradiation (75 W/m^2) without photocatalyst (photolysis). These results confirmed also that the PFOA adsorption on the TiO$_2$ surface was negligible during the photocatalytic reaction.

Further tests were carried out to evaluate the effect of a variation of the photocatalyst concentration in the system. The photoactive power of nanometric titanium dioxide at two different concentrations (0.66 g/L and 1.00 g/L) was evaluated and compared. The corresponding kinetic curves (Fig. 2A) showed a slight general decrease of the mineralization when the concentration of the photocatalyst was increased: after a 6 h treatment, the percentage mineralizations were 30% and 28% and the conversions to fluoride ions were equal to 22% and 21%, respectively. This trend could be explained by the phenomenon of the scattering, due to the amount of catalyst particles dispersed in solution. Finally, the effects due to the variation of the irradiation power were evaluated, testing two different lamp powers: 75 W/m^2 and 95 W/m^2. As expected, the results (Fig. 2B) showed that the photocatalytic efficiency of the system was enhanced by the increase of the power of the incident radiation. In fact, the PFOA percentage mineralization reached

32% after 4 h treatment with the 95 W/m^2 lamp, while in the same conditions, using the 75 W/m^2 lamp, only 21% mineralization was achieved. However, increasing the duration of the test with the 95 W/m^2 lamp, the presence of a limit condition for the photomineralization (*plateau*) in the kinetic curve was noticed: after 6 h treatment the percentage mineralization was still equal to 32%, with a fluoride content of 29%. Conversely, with the 75 W/m^2 lamp a mineralization of 30% and a fluoride content of 15% were obtained after 6 h. Nevertheless, by using the 75 W/m^2 UV-lamp, a similar *plateau* was reached after 9 h UV exposure.

3.2. Analyses of the photocatalyst at different reaction times

IC analysis shows that PFOA degradation reactions generated fluoride ions which could interact with the catalyst; for this reason, P25 was analyzed by XPS before and after the photodegradation reaction (Table 1). Samples collected after 2 h and 4 h of photodegradation presented a substantially constant quantity of fluorine: 25.1%$_{at}$ and 23.9%$_{at}$, respectively. However, a part of the deposited fluorinated compounds was dissolved by suspending a

Table 1
Surface composition (at%) of the catalyst at different reaction times.

Reaction time (h)	Sample	Amount (at%)				OH/O$_{TOT}$ ratio
		Ti	O	F	C	
0	P25	16.3	43.2	–	40.5	0.14
2	–	15.2	39.8	25.3	19.7	0.15
	a.s.[a]	24.0	41.5	12.0	22.5	
4	–	14.7	37.4	23.9	24.0	0.13
	a.s.[a]	17.4	46.6	12.0	24.0	
9	–	22.8	42.5	15.9	18.8	0.71
	a.s.[a]	11.6	51.4	13.6	23.4	

[a] a.s. after suspension (in fluorinated solvent). Before the XPS analysis the sample was suspended in the fluorinated solvent CF$_3$OCFClCF$_2$Cl and dried in inert atmosphere.
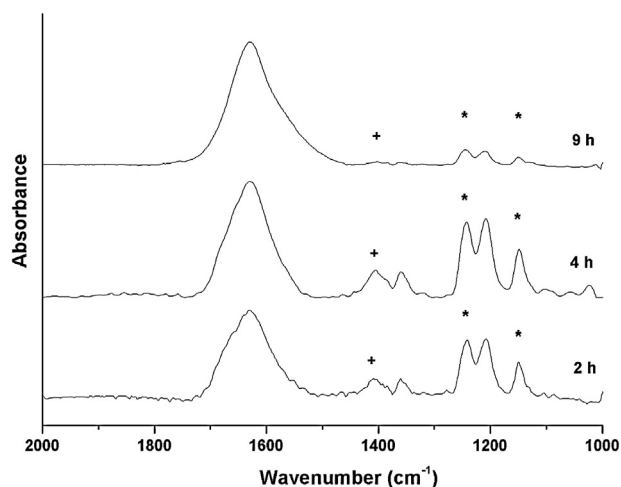
Fig. 3. FT-IR spectra of titanium dioxide catalyst at different reaction times (*) C − F stretching; (+) COO symmetric stretching.

specimen of each sample in the fluorinated solvent $CF_3OCFClCF_2Cl$. As shown in Table 1, the total fluorine content decreased after this treatment to $12.0\%_{at}$ for both the samples collected after 2 h and 4 h.

High resolution XPS spectra were recorded in the typical zone of F 1s signals and showed the presence of two peaks at 684.2 eV and 688.4 eV with almost constant relative areas (85%–90% and 10%–15%) for the samples collected after 2 h and 4 h (see Supplementary information Table 2). The intense signal at 688.4 eV (85%–90%) was due to PFOA molecules and its fluorinated degradation intermediates. These compounds were adsorbed on the catalyst and, as noticed after the suspension in the fluorinated solvent, they can be significantly removed by the fluorinated solvent. The residual part of fluorine (10%–15%) could be attributed to inorganic fluorides. As it is widely reported in literature, small amounts of inorganic fluorides either didn't affect or enhance the photocatalytic properties of titanium dioxide [56]. However, adsorption of reactants to the photocatalyst surface is a critical step in the photocatalytic process [57].

The FT-IR is a highly sensitive method to characterize structural changes of adsorbed species, and the FT-IR spectra of the catalyst at different reaction times are shown in Fig. 3. The broad bands at $1690–1580 \, cm^{-1}$ are assigned to adsorbed water molecules and the strong signals in the range of $1300–1100 \, cm^{-1}$ are attributed to C–F stretching [44]. The symmetric stretching of carboxylate (COO^-) can be observed at $1408 \, cm^{-1}$ [44]. The C–OH vibration at $1210 \, cm^{-1}$ and the asymmetric stretching of carboxylate (COO^-) at $1686 \, cm^{-1}$ were overlaid with absorbance peaks of fluorinated compounds and water, respectively [44]. The peaks due to fluorinated molecules were particularly evident on the samples collected after 2 h and 4 h. However, in the FT-IR spectrum of the sample collected after 9 h these signals were significantly reduced. Similarly, the vibration peak of the symmetric stretching of carboxylate (COO^-) almost disappeared. These results confirmed the presence of PFOA molecules or its fluorinated degradation intermediates on the surface of the catalyst during the photodegradation reaction. After 9 h the mineralization of PFOA that generated fluoride ions was at 32%, but PFOA molecules were not observed on the surface of the photocatalyst.

In order to interpret the high-resolution XPS spectra of TiO_2 samples collected during the photocatalytic process, initial analyses were conducted also on TiF_3, TiF_4 and K_2TiF_6. A summary of the binding energy values obtained through the high resolution analyses of pristine P25 and titanium fluorides is presented in Supplementary information Table 3. For pure sample of TiF_3, TiF_4 and

K_2TiF_6 sharp peaks were observed at 684.7, 685.2 and 686.0 eV, respectively. These peaks can be associated to fluoride ions due to titanium fluoride with different fluorination degree and it can be noticed that the binding energies of the F 1s signals slightly increased as the molar ratio of fluorine atoms in the titanium compounds increased. Thus, the signals at 684.2 eV could be related to titanium fluoride with low degree of fluorination. In the Ti 2p zone, the binding energies of the signals were 459.6–465.4 eV for TiF_3 and 460.4–466.2 eV for TiF_4. The signals of K_2TiF_6 in the Ti 2p zone showed the presence of two species: at 460.4–466.5 eV and at 462.5–468.3 eV.

Significant variations were noticed comparing the catalyst samples collected after 4 h and 9 h of photodegradation. After 9 h of photoabatement, XPS analysis measured a decrease in the fluorine content ($15.9\%_{at}$) on the sample surface, which was barely reduced by suspension in fluorinated solvent ($13.6\%_{at}$). High resolution XPS spectra revealed indeed that the fluorinated organic derivatives due to the PFOA photodegradation were significantly reduced (see Supplementary information Table 2): the signal at higher binding energies (690.8 eV) had in this sample a relative area of just around 50%. The residual fluorine content can be attributed to inorganic titanium-based fluorinated species and a comparison with the XPS spectra of the samples of fluorinated titanium allowed the attributions: the signal at 684.5 eV (~10%) could be related to titanium fluoride with low degree of fluorination, while that at 687.2 eV (~40%) could be due to the formation of highly fluorinated $TiO_{(2-x/2)}F_x$ species during the photoabatement.

High resolution XPS analysis in the zone of Ti 2p signals revealed that pristine titanium dioxide had the double signal of the system Ti $2p_{3/2}$ and Ti $2p_{1/2}$ at 458.6 and 464.3 eV, respectively (see Supplementary information Table 2).

XPS analyses in the Ti 2p region of the catalyst samples obtained at different reaction times showed that no variation occurred on TiO_2 surface in the first four hours of photoabatement (Fig. 4A). The samples collected after 2 h and 4 h revealed values of binding energy and peak distribution almost identical to that of the pristine P25 (see Supplementary information Table 3). Considerable variations were instead noticed comparing the catalyst samples collected after 4 h and 9 h of photodegradation (Fig. 4A and B). After 9 h the XPS spectrum in the Ti 2p region showed three couples of peaks which could be attributed to different titanium fluorides, together with pure titanium dioxide (see Supplementary information Tables 2 and 3): the first couple of peaks, 459.4–464.6 eV, corresponded to TiO_2; the second couple, 460.9–466.0 eV, was probably related to TiF_4; the third couple, finally, 462.0–467.5 eV, might be due to $TiF_6^=$ salts. Overall, it can be observed that the increase in the fluorination degree of the fluorinated titanium compounds gradually shifted the Ti 2p signals towards higher values of binding energies. This behavior can be ascribed to the electron withdrawing properties of fluorine atoms.

The presence of these signals could indicate that the fluoride ions generated during the PFOA abatement interact with the catalytic powder, causing morphological variations on TiO_2 surface and consequently lowering considerably its photoactivity. As widely reported in literature, the incorporation of a moderate amount of fluoride ions to TiO_2 can increase effectively its photocatalytic activity [58–65]. However, variations of reaction operative conditions, especially pH, and use of an excessive molar ratio Ti:F can cause an opposite behavior [66–69]; in particular, as demonstrated by Tressaud et al. [70], the stabilization of F^- ions in the vicinity of Ti^{4+} cations and the limitation of charge carriers mobility totally hinder the photocatalytic activity of TiO_2, whereas titanium hydroxyfluoride species, like $Ti_{0.75}(OH)_{1.5}F_{1.5}$, are formed. An XPS analysis in the Ti 2p region on the catalyst sample collected after 9 h of photodegradation was also repeated after suspension in the fluorinated
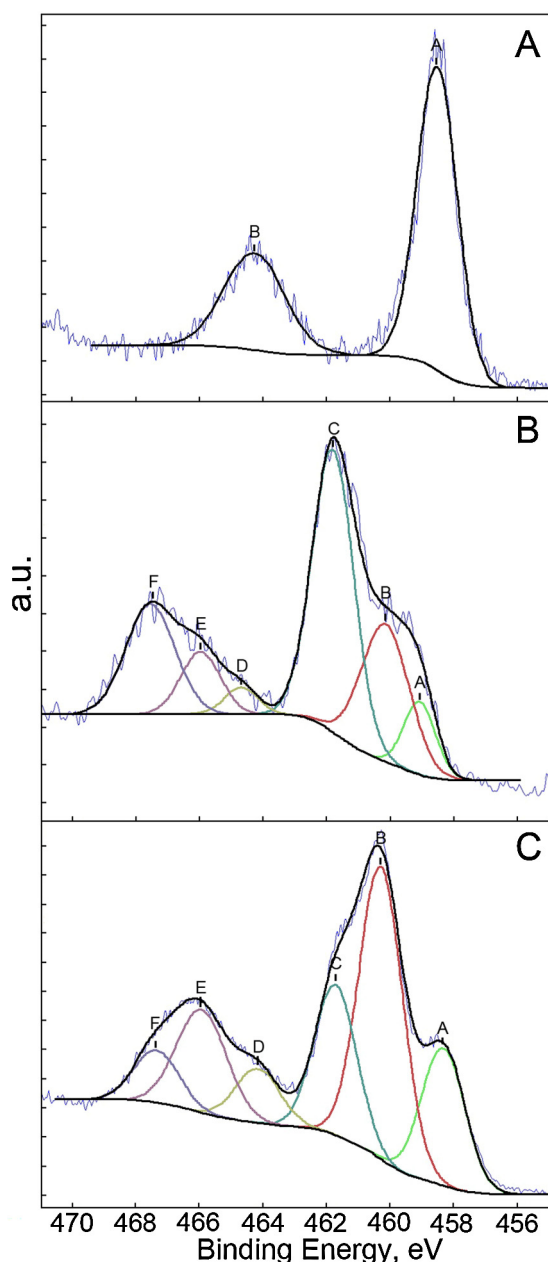
Fig. 4. XPS results—Ti 2p region XPS spectra of titanium dioxide catalyst: after 4 h (A); after 9 h reaction (B); after 9 h reaction and after suspension in fluorinated solvent (C).

Fig. 5. XPS results—O 1s region XPS spectra of titanium dioxide catalyst after 9 h reaction.
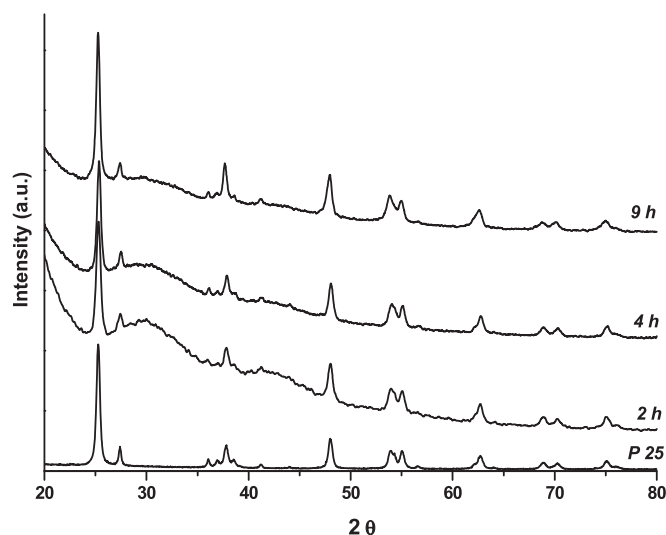
Fig. 6. XRD patterns of titanium dioxide catalyst at different reaction times.

solvent in order to verify if the fluorinated compounds on the surface were effectively bonded to the catalyst or just physically deposited as fluorinated organic compounds (Table 1). As shown in Fig. 4C, the presence of three couples of peaks was confirmed even after this treatment and the binding energies of these signals were comparable with the results presented above: 458.3–464.2 eV, 460.3–465.9 eV and 461.7–467.3 eV. The main difference between the spectra in Fig. 4B and C was represented by an increase in the peaks attributable to TiF_4 to the detriment of the ones ascribable to $TiF_6^=$.

The typical zone of O 1s signals was also monitored by XPS analysis. P25 has a typical signal that can be fitted in two contributions: one at 529.7 eV of the oxygen as oxide and another at 531.4 eV of the hydroxyl groups [56]. The ratio OH/O_{TOT} is around 0.14 (Table 1). Similarly, the XPS analysis of the catalyst samples collected after 2 h and 4 h revealed a signal in the O 1s region with the two
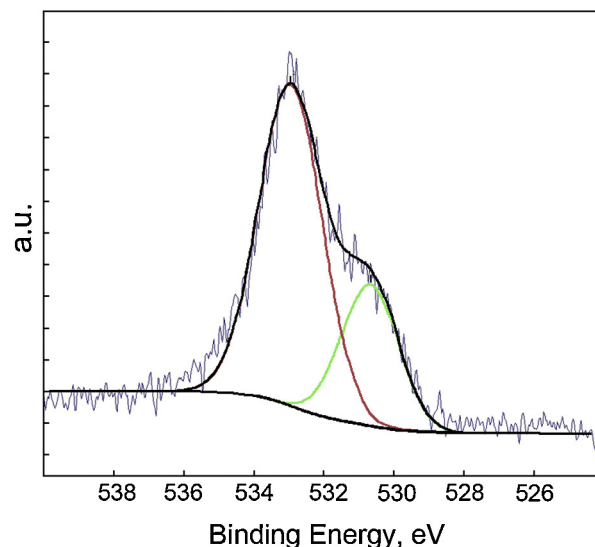
contributions at 529.7 and 531.5 ($\pm$0.1) eV (Supplementary information Table 2). Moreover, the OH/O_{TOT} ratio was approximately the same of that measured on pristine P25 sample: 0.15 after 2 h and 0.13 after 4 h (Table 1). These results corroborated the evidences that the catalyst surface is maintained unchanged during the first four hours of PFOA photodegradation. Conversely, in the O 1s region XPS spectrum of the sample collected after 9 h a peak with two evident contributions at 530.7 and 532.9 eV was observed (Fig. 5). These signals can be attributed again to oxides and hydroxyl groups, respectively, but the number of hydroxyl groups on the catalyst surface was apparently increased: the OH/O_{TOT} ratio in this sample was equal to 0.71 (Table 1). Thus, the chemical modification of the catalyst and, in particular, the substantial formation of highly fluorinated and hydroxylated $TiO_{(2-x/2-y/2)}OH_yF_x$ species on the catalyst surface can be at the basis of the observed limited performances of these photocatalytic process for the PFOA degradation.

In the samples of catalyst collected at different reaction times, X-ray diffraction patterns show the persistence of the typical peaks due to anatase and rutile of P25 titanium dioxide (Fig. 6). In particular, the more intense peak at $2\theta = 25.4°$ is referred to the 101 plane diffraction peak of anatase [56]. XRD spectra were analyzed

with Rietveld method and we observed that anatase crystallites remained almost unaltered (around 25 nm) in the PFOA solution and during the abatement reaction. On the contrary, a size reduction of rutile crystallites from 47 nm to 33 nm can be detected when the photocatalyst is introduced in the PFOA solution. This phenomenon may be reasonably ascribed to a partial transition to an amorphous phase, induced by the acidic and surfactant properties of PFOA. From the XRD results it can be concluded that the anatase crystal phase which have the photocatalytic properties was mainly preserved during the photoabatement of PFOA. As a consequence, the deactivation phenomena can be attributed mainly to variations of the surface chemical composition, as indicated by XPS analysis.

4. Conclusions

The degradation of a common fluorinated surfactant and water pollutant, perfluorooctanoic acid, was studied. The photocatalytic abatement was carried out evaluating several parameters: PFOA concentration related to its CMC, photocatalyst concentration and radiation power of the UV source. The highest degradation rates were obtained working with a concentration of PFOA lower than the critical micelle concentration (CMC), using as photocatalyst nanometric titanium dioxide P25 in concentration 0.66 g/L and high radiation power (95 W/m^2): 32% mineralization of PFOA 0,004 M after 4 h UV exposure was observed. The use of a higher TiO$_2$ concentration (1 g/L) led to worse results, since in these conditions the phenomenon of scattering was increased, affecting the catalyst performances. XRD results revealed that the active anatase phase in the photocatalyst was mainly preserved during the photoabatement of PFOA. The formation of highly fluorinated and hydroxylated TiO$_{(2-x/2-y/2)}$OH$_y$F$_x$ species on the catalyst surface was observed by XPS analysis. Thus, the chemical modification of the catalyst surface induced by fluoride anions can be at the basis of the limited performances of titanium dioxide photocatalyst for PFOA degradation.

Appendix A. Supplementary data

Supplementary data associated with this article can be found, in the online version, at http://dx.doi.org/10.1016/j.apcatb.2013.10.038.

References

[1] E. Smulders, W. von Rybinski, A. Nordskog, Laundry Detergents, in: Ullmann's Encyclopedia of Industrial Chemistry, seventh ed., Wiley-VCH, Weinheim, 2011.
[2] H. Hori, E. Hayakawa, H. Einaga, S. Kutsuna, K. Koike, T. Ibusuki, H. Kiatagawa, R. Arakawa, Environ. Sci. Technol. 38 (2004) 6118–6124.
[3] C.A. Moody, J.A. Field, Environ. Sci. Technol. 34 (2000) 3864–3870.
[4] A. Singh, J.D. Van Hamme, O.P. Ward, Biotechnol. Adv. 25 (2007) 99–121.
[5] US EPA (2002), Revised draft—Hazard assessment of Perfluorooctanoic Acid and its salts, Office of Pollution Prevention and Toxics, Risk Assessment Division, November 4, 2002.
[6] U. Järnberg, K. Holmström, B. van Bavel, A. Kärrman, Perfluoroalkylated acids and related compounds (PFAS) in the Swedish environment—Chemistry Sources & Exposure, Report to Swedish Environment Protection Agency, 2006.
[7] J.G. Drobny, Technology of Fluoropolymers, second ed., CRC Press, Boca Raton, FL, 2009.
[8] C.H. Benson, M.A. Barlaz, D.T. Lane, J.M. Rawe, Waste Manage. 27 (2007) 13–29.
[9] L.E. Doig, K. Liber, Ecotoxicol. Environ. Saf. 66 (2007) 169–177.
[10] A. Mills, N. Elliott, I.P. Parkin, S.A. O'Neill, R.J. Clarke, J. Photochem. Photobiol., A 151 (2002) 171–179.
[11] A. Mills, S. Le Hunte, J. Photochem. Photobiol., A 108 (1997) 1–35.
[12] R. Munter, Proc. Estonian Acad. Sci. Chem. 50 (2001) 59–80.
[13] C. Berberidou, I. Poulios, N.P. Xekoukoulotakis, D. Mantzavinos, Appl. Catal., B 74 (2007) 63–72.
[14] S. Ardizzone, C.L. Bianchi, G. Cappelletti, A. Naldoni, C. Pirola, Environ. Sci. Technol. 42 (2008) 6671–6676.
[15] A. Russo, C. Tonelli, E. Barchiesi, J. Polym. Sci., Part A: Polym. Chem. 43 (2005) 4790–4804.
[16] K. Sato, T. Hirakawa, A. Komano, S. Kishi, C.K. Nishimoto, N. Mera, M. Kugishima, T. Sanoa, H. Ichinose, N. Negishi, Y. Seto, K. Takeuchi, Appl. Catal., B 106 (2011) 316–322.
[17] M.V. Diamanti, M.P. Pedeferri, Corros. Sci. 49 (2007) 939–948.
[18] F. Persico, M. Sansotera, M.V. Diamanti, L. Magagnin, F. Venturini, W. Navarrini, Thin Solid Films 545 (2013) 210–216.
[19] W. Navarrini, M.V. Diamanti, M. Sansotera, F. Persico, M. Wu, L. Magagnin, S. Radice, Prog. Org. Coat. 74 (2012) 794–800.
[20] W. Navarrini, T. Brivio, D. Capobianco, M.V. Diamanti, M.P. Pedeferri, L. Magagnin, G. Resnati, J. Coat. Technol. Res. 8 (2011) 153–160.
[21] S.R. Seagle, Titanium and titanium alloys, in: J.I. Kroschwitz (Ed.), The Kirk Othmer Encyclopedia of Chemical Technology, 24, fourth ed., John Wiley & Sons, New York, 1997, pp. 186–224.
[22] A. Fusjishima, T.N. Rao, D.A. Tryk, J. Photochem. Photobiol., C 1 (2000) 1–21.
[23] M.A. Henderson, Surf. Sci. Rep 66 (2011) 185–297.
[24] A. Zaggia, B. Ameduri, Curr. Opin. Colloid Interface Sci. 17 (2012) 188–195.
[25] M.M. Schultz, D.F. Barofsky, J.A. Field, Environ. Eng. Sci. 20 (2003) 487–501.
[26] G.B. Post, P.D. Cohn, K.R. Cooper, Environ. Res. 116 (2012) 93–117.
[27] B. Ameduri, Chem. Rev. 109 (2009) 6632–6686.
[28] W. Grot, Fluorinated ionomers, in: Plastic Design Library, William Andrew Publishing, Norwich, 2008.
[29] C. Lau, K. Anitole, C. Hodes, D. Lai, A. Pfahles-Hutchens, J. Seed, Toxicol. Sci. 99 (2007) 366–394.
[30] H.J. Lehmler, Chemosphere 58 (2005) 1471–1496.
[31] K. Prevedouros, I.T. Cousins, R.C. Buck, S.H. Korzeniowski, Environ. Sci. Technol. 40 (2006) 32–44.
[32] M. Ylinen, H. Hanhijärvi, P. Peura, O. Rämö, Arch. Environ. Contam. Toxicol. 14 (1985) 713–717.
[33] H. Amii, K. Uneyama, Chem. Rev. 109 (2009) 2119–2183.
[34] C. Fei, J.K. McLaughlin, R.E. Tarone, J. Olsen, Environ. Health Perspect. 115 (2007) 1677–1682.
[35] B.J. Apelberg, F.R. Witter, J.B. Herbstman, A.M. Calafat, R.U. Halden, L.L. Needham, L.R. Goldman, Environ. Health Perspect. 115 (2007) 1670–1676.
[36] C.S. Andersen, C. Fei, M. Gamborg, E.A. Nohr, T.I. Sørensen, J. Olsen, Am. J. Epidemiol. 172 (2010) 1230–1237.
[37] D.M. Lemal, J. Org. Chem. 69 (2004) 1–11.
[38] M. Avataneo, W. Navarrini, U. De Patto, G. Marchionni, J. Fluorine Chem. 130 (2009) 933–937.
[39] Y. Wang, P. Zhang, J. Hazard. Mater. 192 (2011) 1869–1875.
[40] H. Lin, J. Niu, S. Ding, L. Zhang, Water Res. 46 (2012) 2281–2289.
[41] T. Ohno, K. Sarukawa, K. Tokieda, M. Matsumura, J. Catal. 203 (2001) 82–86.
[42] E. Selli, C.L. Bianchi, C. Pirola, G. Cappelletti, J. Hazard. Mater. 153 (2008) 1136–1141.
[43] S. Brosillon, L. Lhomme, C. Vallet, A. Bouzaza, D. Wolbert, Appl. Catal., B 78 (2008) 232–241.
[44] X. Li, P. Zhang, L. Jin, T. Shao, Z. Li, J. Cao, Environ. Sci. Technol. 46 (2012) 5528–5534.
[45] O. Carp, C.L. Huisman, A. Reller, Prog. Solid State Chem. 32 (2004) 33–177.
[46] N.P. Mellott, C. Durucan, C.G. Pantano, M. Guglielmi, Thin Solid Films 502 (2006) 112–120.
[47] P. Pichat, Adsorption and desorption processes in photocatalysis, in: E. Pelizzetti, N. Serpone (Eds.), Homogeneous and Heterogeneous Photocatalysis, Springer, New York/Heidelberg, 1986, pp. 533–554.
[48] S.C. Panchangam, A.Y.C. Lin, J.H. Tsai, C.F. Lin, Chemosphere 75 (2009) 654–660.
[49] H. Hori, A. Yamamoto, E. Hayakawa, S. Taniyasu, N. Yamashita, S. Kutsuna, Environ. Sci. Technol. 39 (2005) 2383–2388.
[50] R. Dillert, D. Bahenemann, H. Hidaka, Chemosphere 67 (2007) 785–792.
[51] S. Kutsuna, H. Hori, Int. J. Chem. Kinet. 39 (2007) 276–288.
[52] C. Kormann, D.W. Bahnemann, M.R. Hoffmann, Environ. Sci. Technol. 25 (1991) 494–500.
[53] M. Sansotera, W. Navarrini, G. Resnati, P. Metrangolo, A. Famulari, C.L. Bianchi, P.A. Guarda, Carbon 48 (2010) 4382.
[54] W.J. De Bruyn, J.A. Shorter, P. Davidovits, D.R. Worsnop, M.S. Zahniser, C.E. Kolb, Environ. Sci. Technol. 29 (1995) 1179–1185.
[55] M. Sansotera, W. Navarrini, M. Gola, C.L. Bianchi, P. Wormald, A. Famulari, M. Avataneo, J. Fluorine Chem. 132 (2011) 1254–1261.
[56] J.C. Yu, J. Yu, W. Ho, Z. Jiang, L. Zhang, Chem. Mater. 14 (2002) 3808–3816.
[57] J. Moser, S. Punchihewa, P.P. Infelta, M. Gratzel, Langmuir 7 (1991) 3012–3018.
[58] J. Yu, L. Shi, J. Mol. Catal.: A: Chem. 326 (2010) 8–14.
[59] Y. Wu, J. Zhang, L. Xiao, F. Chen, Appl. Catal., B 88 (2009) 525–532.
[60] G. Liu, C. Sun, H.G. Yang, S.C. Smith, L. Wang, G.Q. Lu, H.M. Cheng, Chem. Commun. 46 (2010) 755–757.
[61] X. Yang, Y. Wang, L. Xu, X. Yu, Y. Guo, J. Phys. Chem. C 112 (2008) 11481–11489.
[62] J. Kim, J. Lee, W. Choi, Chem. Commun. (2008) 756–758.
[63] H. Zhang, P. Liu, F. Li, H. Liu, Y. Wang, S. Zhang, M. Guo, H. Cheng, H. Zhao, Chem. Eur. J. 17 (2011) 5949–5957.
[64] X. Han, Q. Kuang, M. Jin, Z. Xie, L. Zheng, J. Am. Chem. Soc. 131 (2009) 3152–3153.
[65] H.G. Yang, G. Liu, S.Z. Qiao, C.H. Sun, Y.G. Jin, S.C. Smith, J. Zou, H.M. Cheng, G.Q. Lu, J. Am. Chem. Soc. 131 (2009) 4078–4083.
[66] Y.N. Tan, C.L. Wong, A.R. Mohamed, Asia-Pac. J. Chem. Eng. 7 (2012) 877–885.
[67] M.V. Dozzi, E. Selli, Catal. Today 206 (2013) 26–31.
[68] M. Lewandowski, D.F. Ollis, J. Catal. 217 (2003) 38–46.
[69] T.K. Le, D. Flahaut, D. Foix, S. Blanc, H.K.H. Nguyen, T.K.X. Huynh, H. Martinez, J. Solid State Chem. 187 (2012) 300–308.
[70] A. Demourgues, N. Penin, E. Durand, F. Weill, D. Dambournet, N. Viadere, A. Tressaud, Chem. Mater. 21 (2009) 1275–1283.